Metallogr. Microstruct. Anal. (2016) 5:520–527
DOI 10.1007/s13632-016-0318-5

TECHNICAL ARTICLE

Microstructural Evolution and Carbide Precipitation in a Heat-Treated H13 Hot Work Mold Steel

Mu Lin[1] · Xingfeng Zhao[2] · Lizhan Han[1] · Qingdong Liu[1] · Jianfeng Gu[1]

Received: 28 April 2016 / Revised: 8 October 2016 / Accepted: 12 October 2016 / Published online: 28 October 2016

Abstract The microstructure and carbide precipitation for a H13 hot work mold steel after heat treatment and stabilization treatment at 620 °C for up to 20 h were investigated by optical microscopy, electron backscatter diffraction, and transmission electron microscopy. After solutionization at 1020 °C for 40 min followed by oiling cooling and double tempering at 610 °C for 2 h, lathlike martensitic structure was obtained with various alloyed carbides including Cr-rich $M_{23}C_6$ carbide located at prior austenite grain boundaries or lath boundaries and V-rich MC and Mo-rich M_2C carbides distributed in grain interiors. The heat-treated sample had high strength surpassing 1000 MPa at room temperature and 500 MPa at 650 °C. After stabilization treatment at 620 °C for 20 h, the carbides underwent limited coarsening, particularly for the MC and M_2C carbides, which resulted in excellent resistance to tempering softening for the microstructure as the hardness surpassed 300 HV.

Keywords H13 steel · Microstructure · Heat treatment · Carbide · Characterization

✉ Jianfeng Gu
gujf@sjtu.edu.cn

[1] Institute of Materials Modification and Modelling, School of Materials Science and Engineering, Shanghai Jiao Tong University, Shanghai 200240, People's Republic of China

[2] Hitachi Group, Tokyo, Japan

Introduction

Hot work tool steel H13 (4Cr5MoSiV1) is widely used as tools for die casting, forging, and extrusion, due to its mechanical properties like high hardness (>300 HV) and toughness (A_{kv} > 15 J), good wear resistance, thermocyclic stability, and high elevated temperature strength and ductility.

Die casting of Al alloys requires molds that can maintain mechanical rigidity under harsh working conditions of rapid heating and cooling when interacting with molten Al and cooling medium. The cyclic expansion and compression as well as chemical and mechanical wear on the die surface lead to a combination of thermal fatigue (heat checking), erosion, corrosion, and soldering [1]. These known failure mechanisms largely limit the service life of the die casting. Hence, it is important to improve the mechanical properties of the tool steel used for fabricating die-casting mold. It should be noted that the basic properties, such as strength, tempering resistance, ductility, or toughness, strongly influence the properties of thermal fatigue, wear, and erosion or corrosion that are critical to the final service life of the mold [2]. For example, the yield strength to some extent determines the thermal fatigue resistance. It has been reported that the structure–properties relationship for hot work tool steels is directly related to the various carbides distributed in the tempered martensitic structure [3]. Therefore, it is important to tailor the microstructure and carbide precipitation via the heat treatment and estimate the related tempering resistance and the carbide coarsening at elevated temperature. In this paper, the microstructure and carbide precipitation of H13 are characterized by optical microscopy (OM), electron backscatter diffraction (EBSD), and transmission electron

microscopy (TEM) after heat treatment and stabilization treatment.

Experimental Details

The chemical composition of the H13 tool steel determined by ICP-OES is reported in Table 1. The material underwent austenitization treatment at 1020 °C for 40 min followed by oil cooling and was double-tempered at 610 °C for 2 h followed by air cooling. The heat treatment schedule is shown in Fig. 1. After the heat treatment, the material was reheated to 620 °C and held for up to 20 h to estimate temper resistance of the final microstructure.

The microhardness (HV) was measured with a 200-gf load with a dwell time of 15 s to track the microstructural evolution during heat treatment. The tensile samples with $20 \times 6 \times 1.5$ mm^3 gauge dimensions were tested with a crosshead speed of 0.5 mm/min on a tensile machine at room temperature and at high temperatures of 570, 610, and 650 °C. The yield strength was measured at the 0.2% offset stress. Each hardness or strength was estimated by the average value of three independent measurements with standard deviation.

The microstructure was characterized by optical microscopy, scanning electron microscopy, and electron backscattered diffraction with a field emission scanning electron microscope at 20 kV. The alloyed carbides were characterized by transmission electron microscopy at 200 kV. Thin foils for TEM observation were prepared by mechanical grinding to 50 μm thick followed by electropolishing in a mixture of 95 vol% alcohol and 5 vol% perchloric acid using a double-jet electropolisher with a voltage of 30 V at −30 °C.

Results and Discussion

Hardness Change Versus Microstructure Evolution

Figure 2 shows hardness change in every heat treatment step and then after holding at 620 °C. The as-received sample has comparatively low hardness below 200 HV. After solution treatment at 1020 °C with the following oil cooling, the hardness is substantially increased to as high as approximately 425 HV. The first tempering step further contributes to a short hardness increment, whereas the second one with the same tempering temperature and time slightly leads to decrease in hardness. The heat-treated sample has a hardness surpass 300 HV even after holding for 20 h at 620 °C, which is significantly higher than the received sample in annealed state. This means that the heat-treated sample exhibits excellent resistance to tempering softening. The hardness changes depend on the microstructure evolution as described below.

Figure 3 presents a series of optical images showing the microstructural evolution during the heat treatment. The initial microstructure of the as-received sample in annealed condition consists of ferritic matrix and a dispersion of carbide precipitates, as shown in Fig. 3a. The carbides are generally linearly arranged and thought to be formed associated with austenite–ferrite transformation, i.e., formed by the known interphase precipitation mechanism

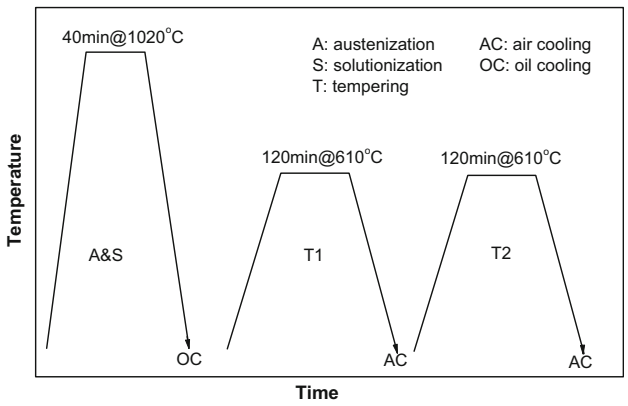

Fig. 1 Schematic illustration of the heat treatment schedule

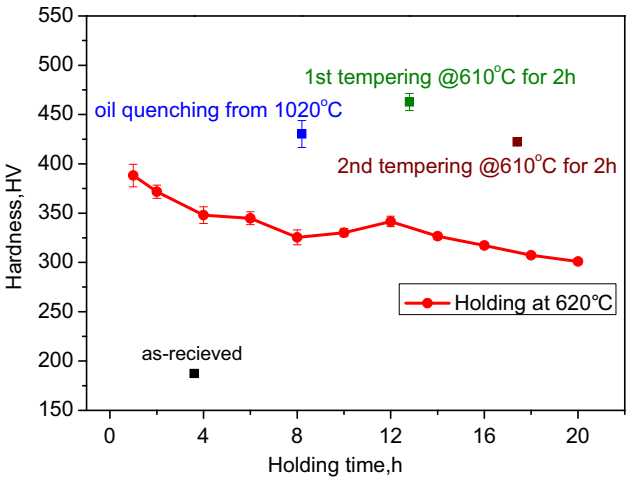

Fig. 2 Hardness evolution in heat treatment and after holding at 620 °C for different time

Table 1 Chemical composition of as-received H13 steel

Elements	C	Si	Mn	Cr	Mo	V	P	S	Fe
wt%	0.37	0.95	0.36	5.13	1.23	0.83	0.009	0.001	Bal.

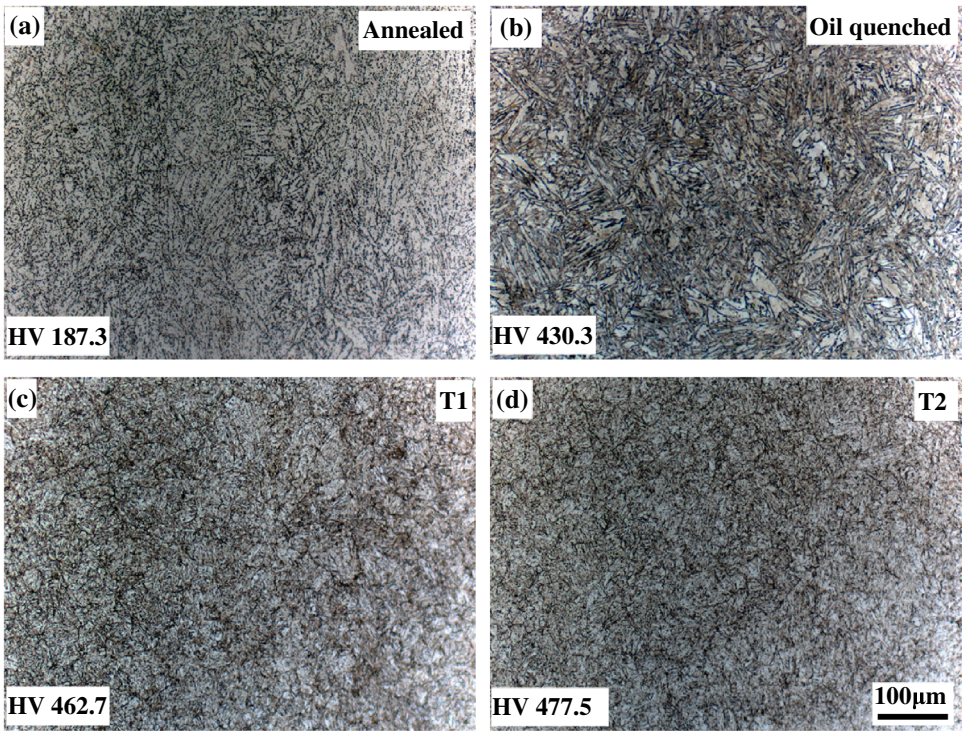

Fig. 3 Optical microstructure of the samples (**a**) as-received, (**b**) solution-treated at 1020 °C for 40 min followed by oil cooling, (**c**) tempered (*T*1) and (**d**) double-tempered (*T*2) at 610 °C for 2 h

[4]. The carbides are clearly observed by optical microscopy, which means most of the carbides have large sizes and thus contribute to relatively weak precipitation strengthening. In addition, the ferritic matrix is comparatively a "soft" phase. Consequently, the as-received sample has a relatively low hardness. After the solution treatment and subsequent oil cooling, the sample has an entirely martensitic structure, as shown in Fig. 3b, because the steel has an excellent hardenability with abundant Cr and Mo additions [5]. Heating at 1020 °C for 40 min permits dissolution of most carbide precipitates containing Cr, Mo, and V, etc., taking the solubility of these carbides into account [6], and related alloying elements are mostly in solid solution in martensitic matrix after the oil cooling, as shown in Fig. 3b. The solid solution strengthening and the dislocated martensite itself yield a relatively high hardness. The sample shows fine microstructure after first tempering at 610 °C for 2 h, and secondary tempering in the same condition does not significantly change the microstructure, as shown in Fig. 3c, d, respectively. Tempering undoubtedly causes softening of the martensitic matrix by reducing the density of crystallographic defects such as dislocations and, therefore, lowers the basic strength. However, more importantly, tempering leads to the extensively carbide precipitation and hence gives rise to substantial precipitation hardening, since the carbides formed during tempering are often dispersedly distributed with high number density and small sizes, as shown by the TEM observation in the following section.

Figure 4 displays the optical images of the heat-treated steel samples after holding at 620 °C from 1 to 20 h. The microstructure generally consists of tempered martensite with a dispersion of carbide precipitates throughout heating at 620 °C. This means the lathlike structure can be kept for a sufficiently long time without any evidence for the occurrence of recovery and crystallization, which is consistent with the small hardness declination during heating at 620 °C as shown in Fig. 2. The stable microstructure is a result of precipitation of various carbides formed during heat treatment, which will be well characterized by TEM observation in the following section.

Tensile Strength

Taking the actual service environment of the steel into account, the high-temperature tensile behavior should be considered and compared with that in room temperature (RT). Figure 5 shows (a) the stress–strain curves and (b) the tensile strength (TS), yield strength (YS), and elongation (EL) varying with the tested temperature. The RT stress–strain curve behaves in a traditional continuous yielding way with the YS exceeding 1000 MPa and TS approaching 1500 MPa as well as an EL of ~14%. The extremely high strength and the moderate ductility are attributed to the martensitic matrix with the dispersion of carbide precipitates as shown in Fig. 3d. At high temperature, the plastic deformation can immediately occur when the stress was applied, leading to strain change at the very

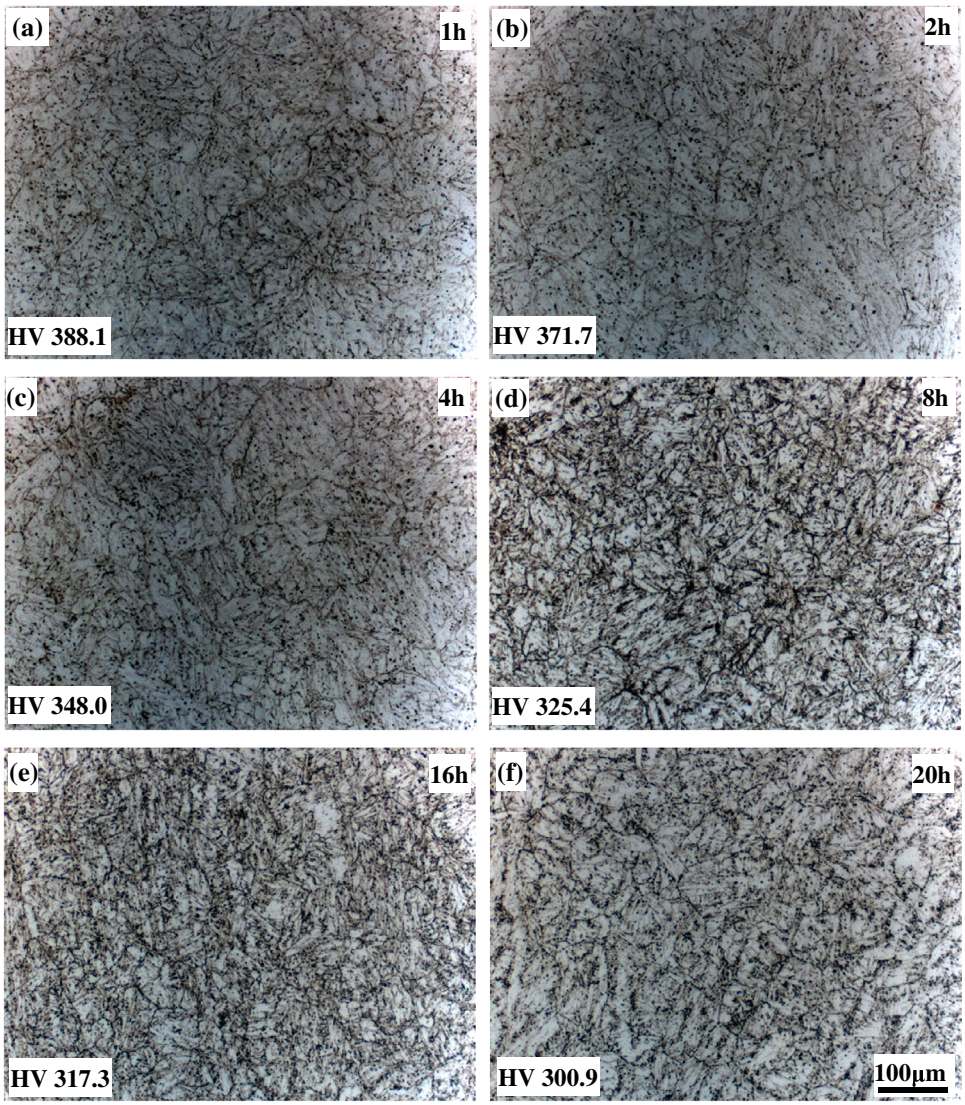

Fig. 4 Optical microstructure of the steel sample solution-treated at 1020 °C for 40 min followed by oil cooling and then double-tempered at 610 °C for 2 h, and then tempering at 620 °C for (**a**) 1 h, (**b**) 2 h, (**c**) 4 h, (**d**) 8 h, (**e**) 16 h, and (**f**) 20 h

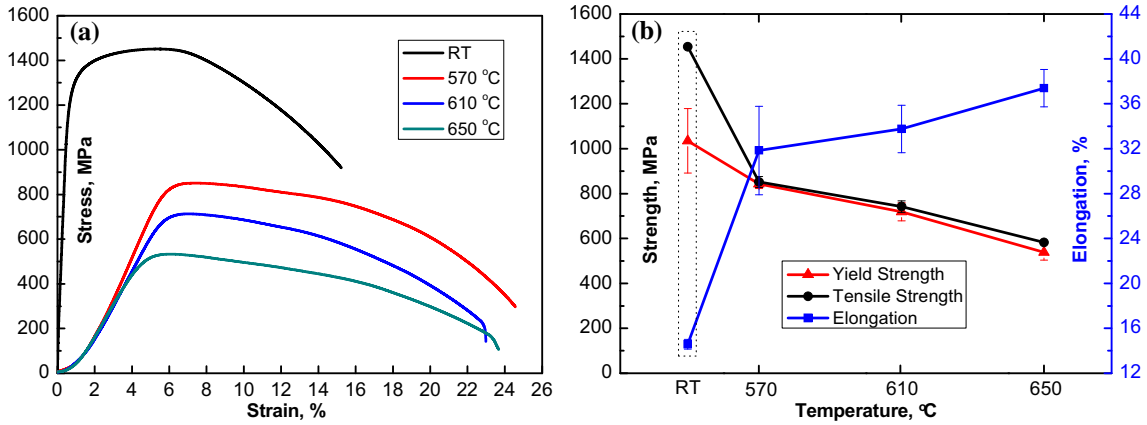

Fig. 5 (**a**) Stress–strain curves and (**b**) mechanical properties of the heat-treated samples tested at room temperature (RT) and different temperatures of 570, 610, and 650 °C

beginning of extra load. The phenomena, which is different from that in RT tensile test, is possibly due to initial strain not requiring continuous accumulation of mobile dislocations to induce yielding. In other words, one can consider the stress–strain curves at high temperature are without elastic deformation. Based on this point, it is also

easy to understand the YS and TS are very close at high temperature as shown in Fig. 4b. This suggests continuous plastic deformation proceeds until the fracture occurs. Compared to that in RT, the strength at high temperature is significantly decreased with increased temperature from 570 to 650 °C. Meanwhile, the EL is increased accordingly manifesting better ductility. It is known that plastic deformation is more dependent on abundant slip system of the matrix at high temperature than that of the dislocation mobility which needs extra energy at RT [7]. In addition, higher temperature means larger carbide precipitates due to more adequate coarsening and more extensive recovery or recrystallization of martensitic structure, which decreases the strength arising from carbide precipitation and dislocated lathlike martensite.

Detail Microstructure of Heat-Treated Sample

EBSD Microstructure

Figure 6 shows the microstructures obtained by SEM-EBSD of the heat-treated sample. After conventional oil quenching from 1020 °C for 40 min and double tempering at 610 °C for 2 h, the lathlike martensitic microstructure is fine-grained (Fig. 6a), as manifested by the prior austenite grain boundaries (PAGBs) which are roughly outlined by the black lines in Fig. 6b with the orientation between 15° and 45°. The appearance of sub-grain boundaries, i.e., the boundaries of martensite packet, block, and lath, substantially reduces equivalent grain sizes. The fine structure, which is a consequence of comparatively low quenching temperature of 1020 °C and carbide precipitation that inhibits the rapid coalescent of grains during double tempering, is responsible for the high strength of the heated-treated sample, as shown in Fig. 5. The orientation image in Fig. 6c indicates the crystals of martensite are generally randomly distributed, which permits the random precipitation of various carbides at the same time.

TEM Microstructure

TEM microstructures of the heat-treated sample are shown in Fig. 7. The typical lathlike structure and shorten lath structure due to tempering recovery are simultaneously observed in Fig. 7a. The distinctly different morphology is separated by a PAGB. In addition, the microstructure has a high dislocation density, which is also clearly shown by the dislocation structure in Fig. 7b. Some small carbide precipitates are seen interacting with the dislocation, and some larger ones are detected located at LBs. After the double tempering, the amounts of retained austenite (RA) are expected to be largely reduced, but some RA can also be found occasionally remaining at LBs, as shown in Fig. 7c. Figure 7d displays the distribution and morphology of various carbide precipitates, which are also found at PAGB (Fig. 7a) and LBs or dislocation (Fig. 7b). In light of the literature on carbide precipitation in this type of steel [8], the spherical and rod-like large carbides located at PAGBs and LBs are Cr-containing $M_{23}C_6$ or M_7C_3 type, which are thought to effectively retard the recovery and recrystallization of the lathlike structure. Nanometer-sized carbides mainly located in the martensitic matrix are considered to be Mo-containing hexagonal M_2C or V-containing cubic MC type, which exert an effective precipitation hardening.

Carbide Evolution After Stabilization Treatment

Figure 8 shows TEM micrographs of the experimental steel after stabilization treatment at 620 °C for 20 h. The lathlike morphology is also seen, but the laths become broad

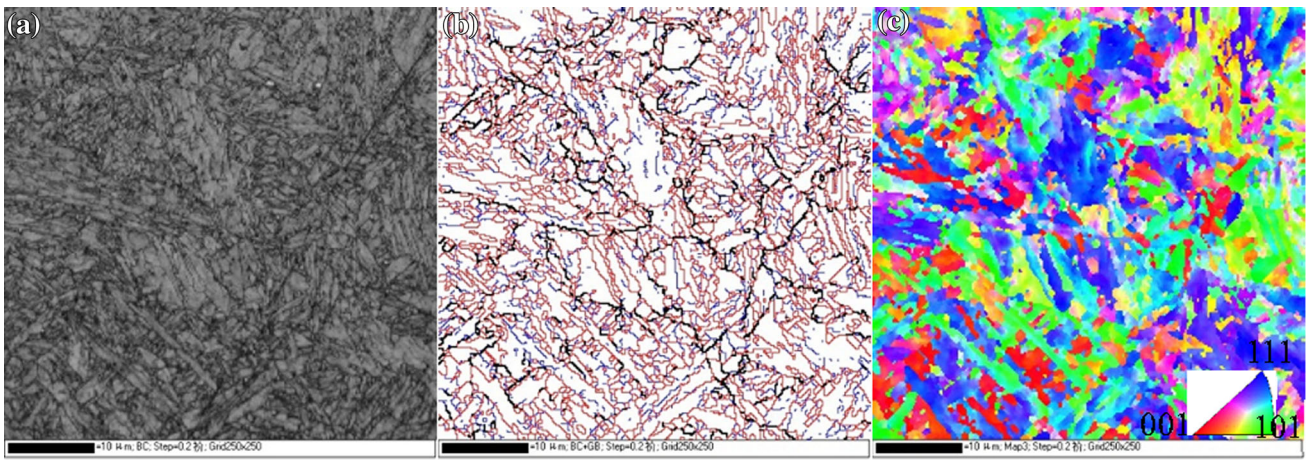

Fig. 6 EBSD images of the heat-treated sample represented by (**a**) image quality map, (**b**) grain boundary map (coloring criterion of boundary: $5° \leqq \theta < 15°$, blue lines; $15° \leqq \theta < 45°$, black lines; $45° \leqq \theta$, red lines), and (**c**) crystal orientation imaging map with colors of different ferritic crystals showing the crystallographic orientations as indicated in the stereographic triangle

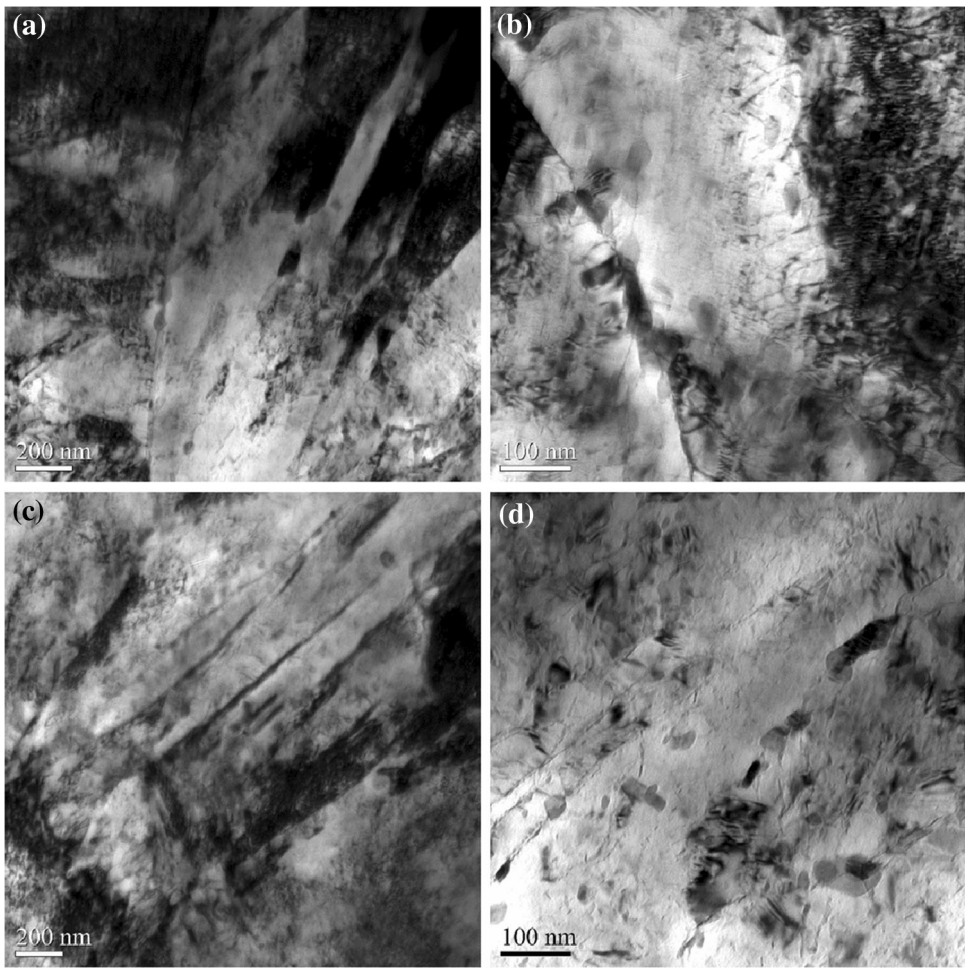

Fig. 7 TEM micrographs of the heat-treated sample, revealing (**a**) lathlike martensite microstructure with high dislocation density, (**b**) small carbide precipitates formed on dislocations and large-size ones at a lath boundary, (**c**) occasionally found retained austenite at martensite lath boundaries, and (**d**) spherical and rod-like large carbides and fine-dispersed needle-like carbide

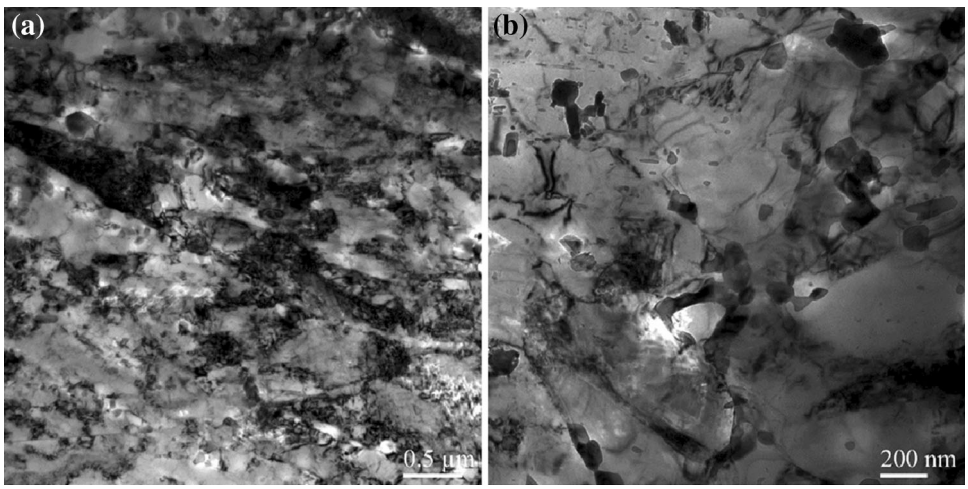

Fig. 8 TEM micrographs of the heat-treated sample after stabilization treatment at 620 °C for 20 h, showing the general morphology of (**a**) partly recovered microstructure and (**b**) coarsened various types of carbide precipitates

and shortened, as shown in Fig. 8a. However, the structure is still highly dislocated as the recovery partly occurs. The degradation of martensitic structure certainly reduces the hardness and strength of the matrix. The distribution morphology of the carbide precipitates is distinctly different from that in heat-treated sample, as shown in Fig. 8b. Most of Cr-containing M_7C_3 and $M_{23}C_6$ carbides located at PAGBs and LBs coarsen to comparatively large size. More complex M_6C carbides with irregular shape are formed based on some preexisting M_7C_3 and $M_{23}C_6$ carbides, leading to the collocated carbides which are not observed in heat treatment condition. The coarsening and

degradation of the type of carbides will depress their precipitation hardening and make the recrystallization of lathlike structure more easily occur. Therefore, the strength contribution of the carbides will be largely reduced. In addition, small M_2C and MC carbides are also detected, but which seem to be still dispersedly distributed and merely a little larger in size than those in the heat-treated sample. This means the carbides have a relatively low growth rate and thus have high resistance to coarsening, because the carbides offer a sufficiently small mismatch with the matrix combined with sufficient thermodynamic stability [9].

Figure 9 shows typical morphology of the coarsened carbides after stabilization treatment. One of the important carbides is $M_{23}C_6$ type carbide, as shown in Fig. 9a. The surrounding martensitic matrix seems to be fully recovered without lathlike structure and dislocation. This type of carbide was formed during tempering, but has comparatively high coarsening rate and grows to large size of approximately 150 nm in diameter during stabilization treatment. Some rod-like carbides with several hundred nanometers long are frequently seen and known as M_2C-type carbides, as shown in Fig. 9b. The carbide is considered as secondary carbide that is formed on the initial Mo-rich M_2C carbide by Cr continuous diffusion within [10]. In addition, a group of carbides arranged in circle is observed, which is thought to be formed during the stabilization treatment by carbide precipitation on a dislocation loop. Figure 9c shows collocated carbides formed during the stabilization treatment. The Mo-rich M_2C or V-rich MC carbide newly nucleates on the preexisting $M_{23}C_6$ and grows in one given direction and evolves to the observed morphology, which is consistent with the previous study [11]. The formation of the carbide pairs possibly impedes the rapid coarsening of $M_{23}C_6$, but, meanwhile, they consume Mo and V which are added to form fine M_2C or MC carbides. Therefore, the appearance of the carbide pairs is not expected because it will prevent extensively formation of nanometer-sized precipitation hardening carbides. Figure 9d shows a square carbide which is not frequently detected. The carbide is thought to be undissolved during solution-treated at 1020 °C. Higher austenitization temperature may dissolve the carbide formed during steel making and therefore release more V and Mo, etc., for stronger precipitation hardening, however, which will also

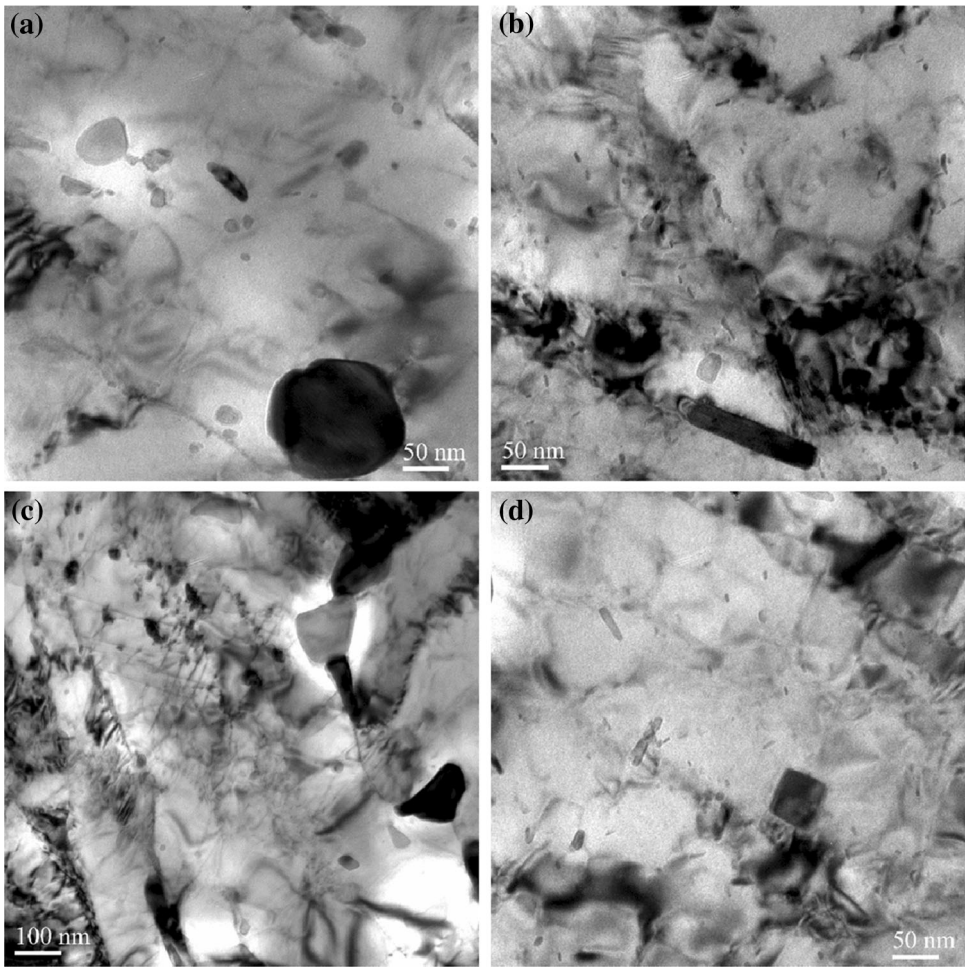

Fig. 9 TEM micrographs of various types of carbides with (**a**) spherical, (**b**) rod-like, (**c**) irregular, and (**d**) square shape. Note that fine precipitates with several nanometer size are widely detected

lead to larger prior austenite grain size. In addition to the carbides that contribute to limited precipitation hardening because of their comparatively large size after stabilization treatment, smaller carbides are also frequently seen, as shown by all images in Fig. 9. The carbides generally have spherical and needle-like morphology for MC and M_2C types, respectively. This suggests this type carbide has very strong stability to temper resistance and is even kept within small size range after stabilization treatment. In consideration of the hardness evolution during tempering at 620 °C shown in Fig. 2, the hardness is not significantly decreased up to 20 h compared to the initial hardness of the heat-treated sample. It is noted that the finely dispersed M_2C and MC carbides other than the M_7C_3 and $M_{23}C_6$ carbides contribute to major precipitation hardening and are decisive of the tempering resistance of the steel.

Summary

The microstructural evolution and hardness change as well as carbide precipitation during heat treatment and stabilization treatment were studied by OM, EBSD, and TEM. The heat treatment schedule consisting of solutionization at 1020 °C for 40 min followed by oiling cooling and double tempering at 610 °C for 2 h results in lathlike martensitic structure with highly dispersed carbide precipitates. The microstructure exhibits excellent resistance to tempering softening as the hardness surpasses 300 HV after holding for 20 h at 620 °C and the strength surpasses 500 MPa at 650 °C. The excellent strength is attributed to high stability of dislocated lathlike martensitic structure and precipitation hardening of nanoscale V-rich MC and Mo-rich M_2C-type carbides (M denotes carbide-forming element), which have relatively low coarsening rate on exposure to high temperature.

References

1. V.V. Ivanov, W.G. Ferguson, I.R. Paine, Study of thermal fatigue of H13 die steel with various surface treatment. Int. J. Mod. Phys. B **17**, 1671–1677 (2003)
2. S. Maim, L.-Å. Norström, Material-related model for thermal fatigue applied to tool steels in hot-work applications. Met. Sci. **13**, 544–550 (1979)
3. L.-Å. Norström, N. Öhrberg, Development of hot-work tool steel for high-temperature applications. Met. Technol. **8**, 22–26 (1981)
4. Q.D. Liu, W.Q. Liu, X.Y. Xiong, Correlation of Cu precipitation with austenite–ferrite transformation in a continuously cooled multicomponent steel: an atom probe tomography study. J. Mater. Res. **27**, 1060–1067 (2012)
5. M.V. Li, D.V. Niebuhr, L.L. Meekisho, D.G. Atteridge, A computational model for the prediction of steel hardenability. Metall. Mater. Trans. B **29**, 661–672 (1998)
6. A. Kroupa, A. Výrostková, M. Svoboda, J. Janovec, Carbide reactions and phase equilibria in low-alloy Cr–Mo–V steels tempered at 773–993 K. Part II: theoretical calculations. Acta Mater. **46**, 39–49 (1998)
7. I. Karaman, H. Sehitoglu, K. Gall, Y.I. Chumlyakov, H.J. Maier, Deformation of single crystal Hadfield steel by twinning and slip. Acta Mater. **48**, 1345–1359 (2000)
8. J. Zhou, D. Ma, H. Chi, Z. Chen, X. Li, Microstructure and properties of hot working die steel H13MOD. J. Iron. Steel Res. Int. **20**, 117–125 (2013)
9. J. Strid, K.E. Easterling, On the chemistry and stability of complex carbides and nitrides in microalloyed steels. Acta Metall. **33**, 2057–2074 (1985)
10. L. Cipolla, H.K. Danielsen, D. Venditti, P.E. Di Nunzio, J. Hald, M.A.J. Somers, Conversion of MX nitrides to Z-phase in a martensitic 12% Cr steel. Acta Mater. **58**, 669–679 (2010)
11. M.I. Isik, A. Kostka, G. Eggeler, On the nucleation of Laves phase particles during high-temperature exposure and creep of tempered martensite ferritic steels. Acta Mater. **81**, 230–240 (2014)